

Supplementary Material of “Mean-field predictions of scaling prefactors match low-dimensional jammed packings”

James D Sartor*, Sean A. Ridout†, Eric I. Corwin*

**Department of Physics and Materials Science Institute,
University of Oregon, Eugene, Oregon 97403, USA*

†Department of Physics and Astronomy University of Pennsylvania, Philadelphia, PA 19104, USA

Measured values of φ_j

In Table I we show our measured values of φ_j . these values are used in calculating $\Delta\varphi$.

Table I: Measured values of φ_j in dimensions 2-10.

d	2	3	4	5	6	7	8	9	10
φ_j	0.85	0.65	0.46	0.31	0.20	0.13	0.078	0.049	0.029

MEAN FIELD PREDICTIONS OF PREFACTORS

Mean Field Prediction of Pressure vs Packing Fraction

Mean field theory predicts that pressure scales with packing fraction as follows [S1]:

$$\hat{P} = \hat{C}(\hat{\varphi} - \hat{\varphi}_j) \quad (S1)$$

where $\hat{C}_{p\varphi}$ is a constant, and the hats over P and $\Delta\varphi$ signify that the quantities are scaled such to be fixed in the infinite dimensional limit, as follows:

$$\hat{P} = \frac{P^*}{\rho d} \quad (S2)$$

$$\hat{\varphi} = \frac{2^d}{d} \varphi \quad (S3)$$

where ρ is the number density, $\frac{N}{V}$, and P^* is the pressure which is calculated with assumed unit particle diameter. This relates to our pressure, P , as follows:

$$P = \frac{\varphi}{\rho} \frac{1}{d^2} P^*, \quad (S4)$$

where the factor of $\frac{\varphi}{\rho}$ unwraps their assumption of unit particle diameter, and the factor of $\frac{1}{d^2}$ comes from their potential, which explicitly contains a dimensional term:

$$U^*(r) = \frac{\epsilon d^2}{2} \left(\frac{r}{\ell} - 1 \right)^2 \Theta(\ell - r). \quad (S5)$$

We can thus rewrite equation S2 in terms of our pressure P :

$$\hat{P} = \frac{d}{\varphi} P, \quad (S6)$$

and therefore equation S1:

$$\frac{d}{\varphi}P = \hat{C} \frac{2^d}{d} (\varphi - \varphi_j) \quad (\text{S7})$$

$$P = \frac{\varphi}{d} \hat{C} \frac{2^d}{d} \Delta\varphi \quad (\text{S8})$$

$$P = \frac{1}{d} \hat{C} \hat{\varphi}_j (\Delta\varphi) \quad (\text{S9})$$

$$P = \frac{1}{d} \hat{C}_{p\varphi} (\Delta\varphi). \quad (\text{S10})$$

Where, noting that $\hat{\varphi}_j$ and \hat{C} are constants in the infinite dimensional limit, we combine them as $\hat{C}_{p\varphi}$. Thus mean field predicts a simple $1/d$ scaling of the prefactor between pressure and excess packing fraction.

Mean Field Prediction of Pressure vs Number Of Excess Contacts

The number of contacts, z , is predicted by mean field theory to have the form [S1]:

$$\frac{z}{2d} = 1 + \hat{C}_{z\varphi} \sqrt{\hat{\varphi} - \hat{\varphi}_j} \quad (\text{S11})$$

$$\frac{z}{2d} = 1 + \hat{C}_{z\varphi} \sqrt{\frac{2^d}{d}} \sqrt{\varphi - \varphi_j} \quad (\text{S12})$$

for some constant $\hat{C}_{z\varphi}$.

The number of excess contacts, δz , therefore is predicted to scale as follows:

$$\frac{\delta z}{2d} = \hat{C}_{z\varphi} \sqrt{\frac{2^d}{d}} \sqrt{\varphi - \varphi_j} \quad (\text{S13})$$

$$\delta z = 2d \hat{C}_{z\varphi} \sqrt{\frac{2^d}{d}} \sqrt{\varphi - \varphi_j}. \quad (\text{S14})$$

Mean Field Prediction of Packing Fraction vs Number of Excess Contacts

By combining equations 10 and 14, we can also predict the relation between δz and P :

$$\delta z = 2d \hat{C}_{z\varphi} \sqrt{\frac{2^d}{d}} \sqrt{\frac{d}{\hat{C}_{p\varphi}} P} \quad (\text{S15})$$

$$= 2d \hat{C}_{z\varphi} \sqrt{\frac{2^d}{\hat{C}_{p\varphi}}} \sqrt{P} \quad (\text{S16})$$

$$(\text{S17})$$

where we define $\hat{C}_{zp} = \frac{2\hat{C}_{z\varphi}}{\sqrt{\hat{C}_{p\varphi}}}$.

Excess Contacts vs Excess Packing Fraction Prefactor Scaling

From eqns 5 and 6 we can simply relate δz and φ as follows:

$$\delta z = C_{z\varphi} (\Delta\varphi)^{1/2} \quad (\text{S18})$$

where clearly,

$$C_{z\varphi} = C_{zp} \sqrt{C_{p\varphi}}. \quad (\text{S19})$$

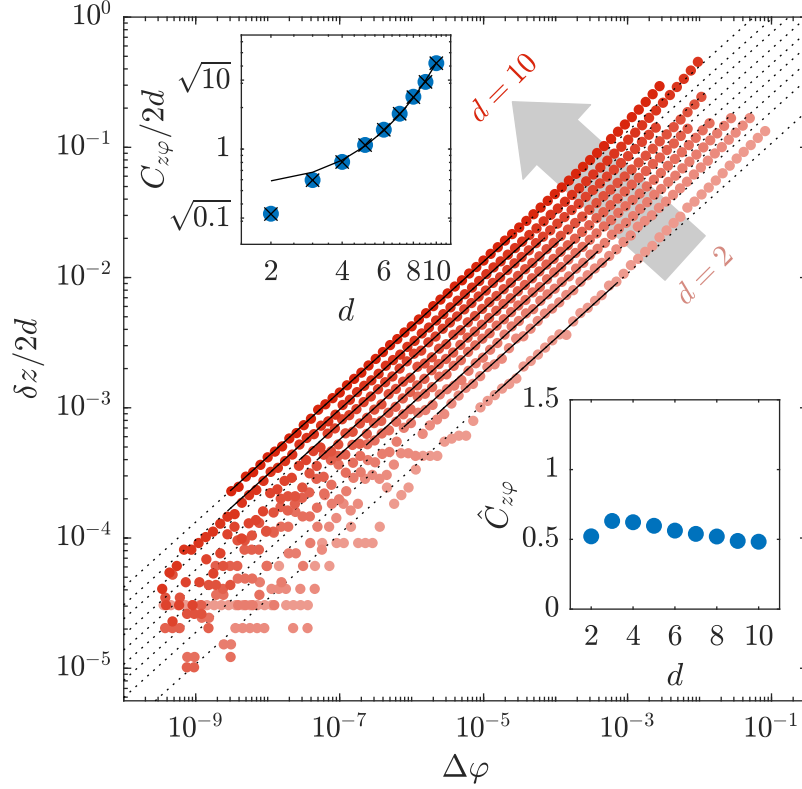


Figure S1: Measured excess contacts scales with the square root of excess packing fraction for systems from $d = 2$ to $d = 10$ (red circles). Black lines show the fits for C_{zp} using eqn S18. For our fits, we ignore data at high pressure and low contact number as in figure 2. Dotted lines show the extension of our fits beyond the fitted range. Inset shows the measured values of $C_{z\varphi}$ (blue circles), which scale in agreement with the mean field prediction eqn S14 using measured values of $\hat{C}_{z\varphi} \approx 0.83$. Additionally, to note consistency we show that our measured values of $C_{z\varphi}$ agree well with values calculated from our measurements of $C_{p\varphi}$ and C_{zp} using eqn S19 (black x's).

In figure S1, we show this scaling separately for each dimension. We fit each line to eqn S18 to find the values of the prefactor $C_{z\varphi}$ in each dimension, the values of which are shown in the inset. These values agree well with both the mean field prediction above $3D$, shown as a black line, and our calculated value from C_{zp} and $C_{p\varphi}$, shown as black x's in figures 1 and 2.

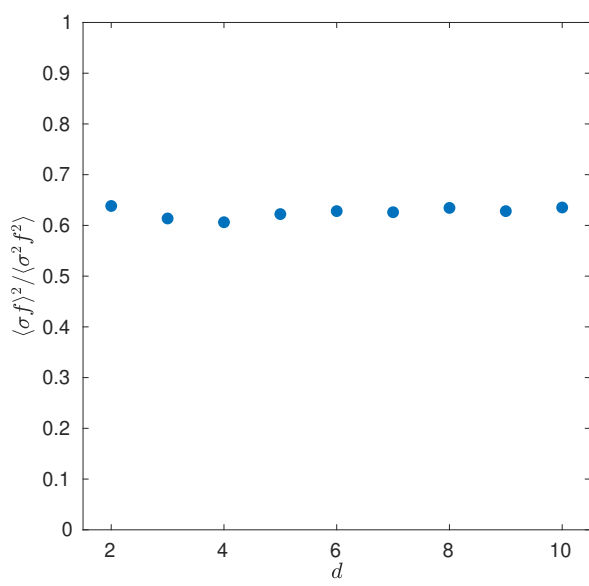
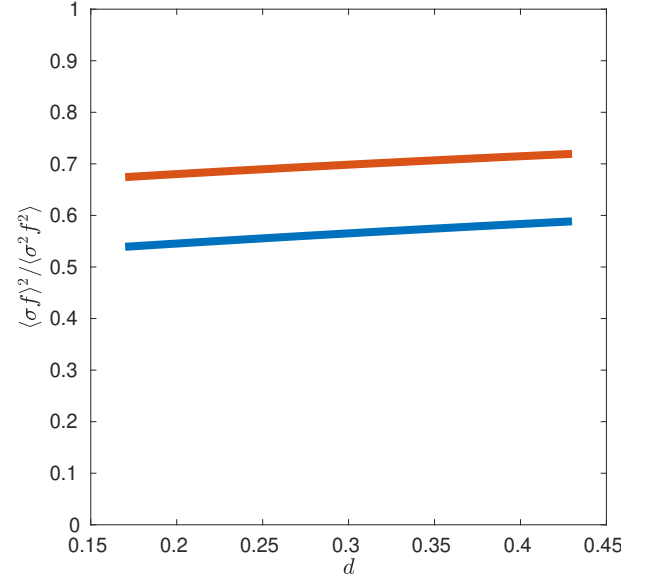
Dimensional Dependence of Force Moment Ratios

In figure S2a we show that the ratio of force moments does not depend strongly on dimension. This empirical fact may seem at odds with previous reports of how the low-force part of the distribution differs from its mean-field form in low dimensions [S2, S3]. The low-force part of the distribution has $P(f) \propto f^\theta$, where $\theta \approx 0.17$ in $d = 2$ smoothly rises to a $d = \infty$ value of $\theta \approx 0.42$. The high-force behaviour decays like an exponential or a stretched exponential; thus, we have computed the theoretical value of this moment ratio for distributions of the form $P(f) \sim f^\theta e^{-f/f_0}$ and $P(f) \sim f^\theta e^{-f^2/f_0^2}$, as shown in figure S2b. We find that neither of these assumed distributions quantitatively predicts the measured moment ratio for the known values of θ , but they do show that the known variation in θ should not make us expect a large variation in this moment ratio.

Accounting for Polydispersity in Pressure vs. Packing Fraction Scaling

To account for the case with varying spring constants we also form the matrix of inverse spring constants

Figure S2: Dimensional dependence of force moment ratios

(a) Dimensionless moment ratio of first and second moments of σf shows no dimensional dependence(b) Neither the force distribution $f^\theta e^{-f/f_0}$ (blue) nor the distribution $f^\theta e^{-f^2/f_0^2}$ (red) predicts a strong θ dependence for the relevant moment ratio

$$k^{-1} = \frac{1}{2\varepsilon} \begin{pmatrix} \sigma_{ij}^2 & & \\ & \ddots & \\ & & \sigma_{kl}^2 \end{pmatrix}. \quad (\text{S20})$$

and the projection operator onto the states of self stress

$$S = \sum_{i=1}^{N\Delta z} |s_i\rangle \langle s_i|. \quad (\text{S21})$$

In terms of these quantities, the bulk modulus may be written as [S4–S6]

$$\frac{\partial^2 E}{\partial V^2} = \frac{1}{V} \langle E | S (S (k^{-1}) S)^{-1} S | E \rangle. \quad (\text{S22})$$

In the one SSS approximation, we can evaluate the two projected quantities that we need to evaluate equation S22. Equations 10 and 12 give

$$S | E \rangle = \langle s_0 | f | s_0 \rangle = \frac{\langle r | f \rangle}{d \sqrt{\langle f | f \rangle}} | s_0 \rangle = \sqrt{Z} \frac{\langle r f \rangle}{d \sqrt{\langle f^2 \rangle}} | s_0 \rangle, \quad (\text{S23})$$

and equations S20 and 12 give

$$S k^{-1} S = | s_0 \rangle \langle s_0 | k^{-1} | s_0 \rangle \langle s_0 | = | s_0 \rangle \frac{\langle \sigma^2 f^2 \rangle}{2\epsilon \langle f^2 \rangle} \langle s_0 | \quad (\text{S24})$$

$$(S k^{-1} S)^{-1} = | s_0 \rangle \frac{2\epsilon \langle f^2 \rangle}{\langle \sigma^2 f^2 \rangle} \langle s_0 | \quad (\text{S25})$$

Furthermore at lowest order in P we have $|r\rangle = |\sigma\rangle$, and we may assume $Z \approx dN$. Thus, equation S22 reduces to

$$K = \frac{2N\varepsilon}{dV} \frac{\langle \sigma f \rangle^2}{\langle \sigma^2 f^2 \rangle}, \quad (\text{S26})$$

and thus via equation 9:

$$C_{p\varphi} = \frac{2}{d} \frac{\langle \sigma f \rangle^2}{\langle \sigma^2 f^2 \rangle}. \quad (\text{S27})$$

Prestress Comparison

It has recently been suggested the relationship between prestress and number of excess contacts collapses perfectly when compared across dimensions [S7]. We define prestress e as in ref. [S7] as:

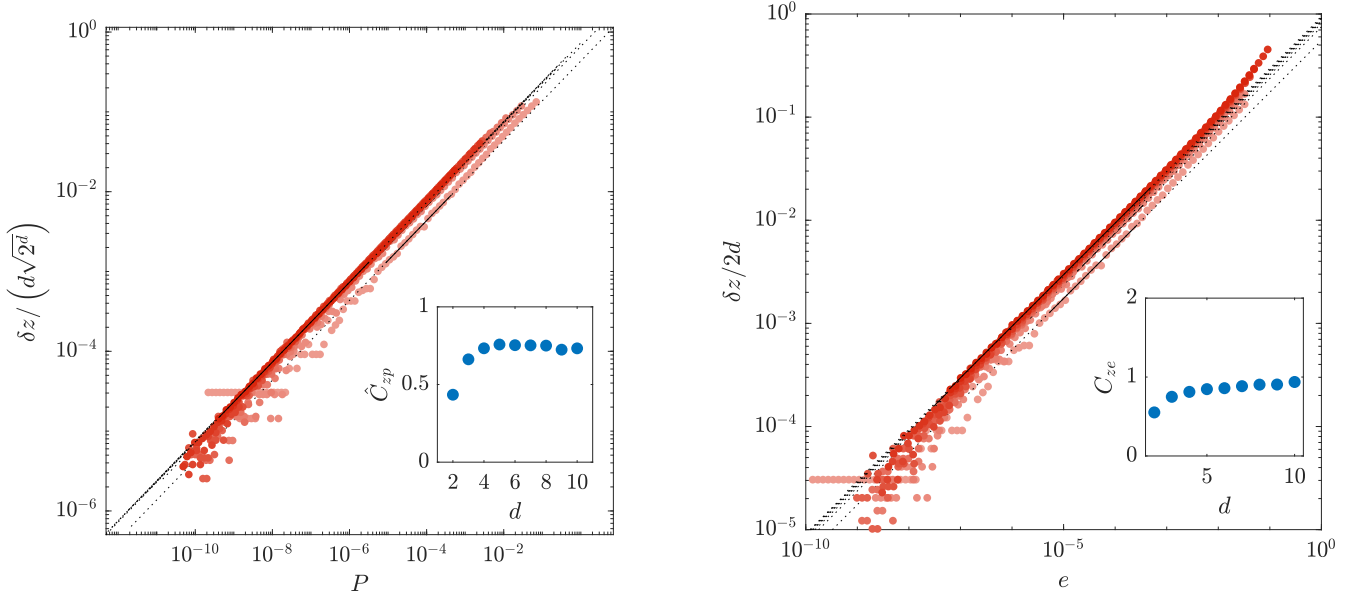
$$e = (d-1) \left\langle \frac{-V'(r_{ij})}{r_{ij} V''(r_{ij})} \right\rangle_{ij} \quad (\text{S28})$$

and expected to scale as:

$$\delta z = C_{ze} e^{\frac{1}{2}} \quad (\text{S29})$$

because it is proportional to pressure near the jamming transition [S7]. In figure S3, we examine the collapse of scaled excess contacts with prestress (fig. S3b), and compare it to the collapse of excess contacts scaled by the mean field prediction with pressure (fig. S3a). In figure S3b we see that the collapse with prestress is not quite perfect - there is a clear upward trend. This stands in contrast to the inset of figure S3a, which shows \hat{C}_{zp} to be nearly constant above three dimensions.

Figure S3: Comparison of scaled excess contacts with pressure and prestress.



(a) Scaled excess contacts scales with the square root of pressure as in figure 2. However, with excess contacts scaled by the expected mean field prediction, eqn. 8, the data collapse onto a single line. The inset confirms the collapse, showing \hat{C}_{zp} to be nearly constant.

(b) Scaled excess contacts scales with the square root of prestress for systems from $d = 2$ to $d = 10$. Black lines show the fits for C_{ze} using eqn S29. The fits ignore high and low pressure data as in figure 2. Lower inset shows the measured values of C_{ze} which have a clear upward trend.

In fact, close to jamming so that $r \approx \sigma$ and $Z \approx Nd$, our dimensionless pressure P as defined in equation 4 is related to the prestress by

$$P = \frac{\bar{V}_p}{\varepsilon V d} \sum_{i,j} \mathbf{f}_{ij} \cdot \mathbf{r}_{ij} \quad (\text{S30})$$

$$= \frac{\bar{V}_p}{\varepsilon V d} Z \langle f_{ij} r_{ij} \rangle_{ij} \quad (\text{S31})$$

$$= \frac{2\varphi Z}{d} \left\langle \frac{r_{ij}}{\sigma_{ij}} \left(1 - \frac{r_{ij}}{\sigma_{ij}} \right) \right\rangle_{ij} \quad (\text{S32})$$

$$= \frac{2\varphi Z}{d} \left\langle \frac{-r_{ij} V'(r_{ij})}{\sigma_{ij}^2 V''(r_{ij})} \right\rangle_{ij} \quad (\text{S33})$$

$$\approx 2 \frac{\varphi_J}{d-1} e. \quad (\text{S34})$$

Thus, our better-fitting form for the $z - P$ relationship amounts to the statement that

$$\frac{\Delta z}{2d} = \hat{C}_\varphi \sqrt{\frac{d}{d-1}} \sqrt{e}. \quad (\text{S35})$$

Thus our scaling forms agree with the statement of reference [S7] in the infinite- d limit, although we see better fit with our form in low dimensions.

-
- [S1] Giorgio Parisi, Pierfrancesco Urbani, and Francesco Zamponi, *Theory of Simple Glasses: Exact Solutions in Infinite Dimensions* (Cambridge University Press, New York, 2020).
- [S2] Patrick Charbonneau, Eric I. Corwin, Giorgio Parisi, and Francesco Zamponi, “Jamming Criticality Revealed by Removing Localized Buckling Excitations,” *Physical Review Letters* **114** (2015), 10.1103/PhysRevLett.114.125504.
- [S3] Daniel M. Mueth, Heinrich M. Jaeger, and Sidney R. Nagel, “Force distribution in a granular medium,” *Physical Review E* **57**, 3164–3169 (1998).
- [S4] S. Pellegrino, “Structural computations with the singular value decomposition of the equilibrium matrix,” *International Journal of Solids and Structures* **30**, 3025–3035 (1993).
- [S5] M. Wyart, “On the rigidity of amorphous solids,” *Annales de Physique* **30**, 1–96 (2005).
- [S6] T C Lubensky, C L Kane, Xiaoming Mao, A Souslov, and Kai Sun, “Phonons and elasticity in critically coordinated lattices,” *Reports on Progress in Physics* **78**, 073901 (2015).
- [S7] Masanari Shimada, Hideyuki Mizuno, Ludovic Berthier, and Atsushi Ikeda, “Low-frequency vibrations of jammed packings in large spatial dimensions,” *arXiv:1910.07238 [cond-mat]* (2019), arXiv: 1910.07238.